Acetylated Microfibrillated Cellulose as a Toughening Agent in Poly(lactic acid)

Mindaugas Bulota,[1] Kätlin Kreitsmann,[2] Mark Hughes,[1] Jouni Paltakari[1]

[1]*Department of Forest Products Technology, School of Chemical Technology, Aalto University, P. O. Box 16400, Aalto 00076, Finland*
[2]*Department of Polymer Materials, Faculty of Chemical and Materials Technology, Tallinn University of Technology, Ehitajate tee 5, Tallinn 19086, Estonia*

Received 22 November 2011; accepted 9 January 2012
DOI 10.1002/app.36787
Published online in Wiley Online Library (wileyonlinelibrary.com).

ABSTRACT: Composites from poly(lactic acid) (PLA) and acetylated microfibrillated cellulose (MFC) were prepared by a solvent casting technique. MFC, mechanically isolated from never-dried bleached birch Kraft pulp, was used as a reinforcement. The acetylation reaction was carried out at 105°C in toluene and proved to be an effective way of increasing the dispersion of MFC in a nonpolar solution of PLA in chloroform. The maximum acetyl content (10.3%) was achieved after 30 min of reaction time. This could be translated to a degree of substitution (DS) of 0.43. The acetylation was confirmed by Fourier transform infrared spectroscopy. MFC with a higher DS exhibited a more pronounced effect on the properties of PLA. Mechanical testing showed that Young's modulus increased by approximately 70% and the tensile strength increased by approximately 60% at a fiber weight fraction of 20%. At an MFC loading of 10 wt %, the strain at break and toughness, expressed as the work of fracture, increased by around 500%. The Young's modulus increased by approximately 15%, whereas the tensile strength remained the same. © 2012 Wiley Periodicals, Inc. J. Appl. Polym. Sci. 000: 000–000, 2012

Key words: composites; fibers; toughness; Raman spectroscopy

INTRODUCTION

Interest in cellulose-reinforced poly(lactic acid) (PLA) composites has been growing over the past decade or so with the number of published scientific articles increasing annually. Lactic acid, the raw material for PLA, can be derived from renewable resources, such as corn or potato starch,[1] and with the demand for environmentally friendly products rising, this makes it a very attractive material. The utility of PLA could, however, be extended into new application areas if its intrinsic brittleness could be reduced. There have been several reports on studies aimed at enhancing the toughness and the strain at break of PLA with cellulose,[2,3] although in these cases, the strain at break did not exceed around 15%, and the composites remained relatively brittle. Other work has demonstrated that the addition of microfibrillated cellulose (MFC) can enhance the toughness. An increase in the fracture energy of nearly 200%, accompanied by a strain to failure of 5%, was reported for a hybrid composite of bamboo and PLA[3] on the addition of 1 wt % MFC. In another study, the addition of 2 wt % MFC to an epoxy matrix was found to result in an increase of 80% in the interlaminar initiation fracture toughness of a plain woven carbon-fiber-reinforced epoxy composite.[4] Similar findings have been reported for carbon-fiber-reinforced epoxy modified with 10 wt % carboxyl-terminated liquid butadiene acrolynitrile upon the addition of 0.5 and 1 wt % MFC[5] and 0.5 wt % bacterial cellulose (BC).[6] Interestingly, the toughening effect was also observed in composites without liquid rubber. The increase in toughness in the aforementioned epoxy composites was attributed to crack deflection due to the incorporation of nanofibrils on the basis of conclusions from an earlier work by Faber and Evans.[7]

MFC is a promising modifier because it has good mechanical properties,[8–10] and because it is derived from woody biomass, it is both abundant and renewable. However, the dispersion of cellulose is difficult in nonpolar or low-polar media[11,12] such as PLA. One way to improve its dispersion in and compatibility with PLA is through surface modification. Acetylation of the polar cellulose hydroxyl groups has been reported as being effective in this respect.[13–16] During the acetylation reaction, the primary hydroxyl groups are esterified (Fig. 1).

Aggregation of the cellulose fibrils due to hydrogen bonding is hindered by the introduction of

Correspondence to: M. Bulota (mindaugas.bulota@aalto.fi).
Contract grant sponsor: Academy of Finland; contract grant number: 127609.

Figure 1 Reaction of the acetic anhydride with a primary cellulose hydroxyl group.

acetyl groups, although this, as well as the dispersion, is strongly dependent on the degree of substitution (DS) of the hydroxyl groups.[17] Acetylation has been shown to improve the dispersion of cellulose nanowhiskers[2,16,18] and MFC[17,19] in a PLA matrix. Moreover, acetylation has been shown to improve the compatibility between wood flour,[20] bacterial cellulose, and eucalyptus bleached Kraft pulp[21] and PLA. Furthermore, acetylation has been shown to lead to the enhanced impregnation of bacterial[14,22] and wood cellulose[23] films and a lower degree of cellulose aggregation.

The aim of the study reported herein was to investigate the potential of acetylation to enhance the mechanical properties, in particular, the toughness, of MFC-reinforced PLA composites. It was shown that the mechanical properties of MFC-reinforced PLA could be dramatically altered by the inclusion of relatively low amounts of acetylated MFC and that the effects were closely related to the DS of the primary alcohols.

EXPERIMENTAL

Materials

MFC was prepared from elemental chlorine-free bleached birch Kraft pulp. The MFC was disintegrated with an ultrafine friction grinder Masuko Supermasscolloider, model MKZA 10-15 (Kawaguchi, Japan) without any chemical treatment. A never-dried pulp suspension was diluted to a 3 wt % consistency and passed through the grinder seven times over a period of approximately 5 h. The final MFC suspension was in the form of a gel and had a solid content of approximately 2 wt %.

The matrix material used in the composite preparation was NatureWorks 2002D PLA (NatureWorks, Minnetonka, MN).

Atomic force microscopy (AFM)

MFC suspensions of approximately 0.015 wt % in water were centrifuged (10,400 rpm for 1 h at 24°C), and the supernatant was spin-coated on a mica substrate (3000 rpm for 1 min at room temperature). The films were imaged in tapping mode with a Nanoscope IIIa multimode scanning probe AFM (Digital Instruments, Inc., Santa Barbara, CA). Silicon cantilevers (NSC15/AIBS, MicroMasch, Tallin, Estonia) were used to perform the imaging at a frequency of 300–360 kHz. The radius of the tips, according to the manufacturer, was about 10 nm.

Acetylation of MFC

A degassed water suspension of MFC (60 g, 2 wt %) was solvent exchanged, by centrifugation (8000 rpm at 20C, 15 min), first to ethanol and then to toluene. The suspensions were sonicated for 2 min before and after the final centrifugation. Acetic anhydride (100 g) was added to 100 g of the MFC suspension in toluene (ca. 1.5 g of dry cellulose). The reaction was conducted at a temperature of 105 ± 5°C for 15 and 30 min. The reaction was quenched by the placement of the reaction flask into an ice bath. Subsequently, 100 g of acetone was added, the mixture was centrifuged, and the remaining reagent, acetic acid byproduct, and solvents were decanted off. Additional acetone (100 g) was added, and the suspension left overnight, after which it was solvent-exchanged to acetone and from acetone to chloroform by centrifugation, as mentioned previously. The final acetylated MFC suspension in chloroform had a concentration of about 1.0 wt %.

Determination of the acetyl content and DS by saponification

The acetyl content was determined with a standard saponification procedure,[24] also known as the *Eberstadt method*. An acetylated MFC suspension in chloroform (50 g) was dried in a fume hood at room temperature and then oven-dried at 105 ± 3°C for at least 2 h. Approximately 0.5 g of dry acetylated MFC was placed in a flask, and 8 mL of 75% ethanol was added. Then, the mixture was heated for 30 min at 60°C. Following this, 8 mL of a 0.5*N* sodium hydroxide (NaOH) solution was added, and the mixture was heated at 60°C for 15 min. The flask was stoppered tightly and left to stand at room temperature for 72 h. Then, the NaOH was titrated with 0.5*N* hydrochloric acid (HCl) with phenolphthalein as an indicator. At the point where the indicating pink color disappeared, an excess 1 mL of 0.5*N* HCl was added, and the mixture was allowed to stand overnight. The small excess of acid was then back-titrated with a 0.5*N* NaOH solution to the phenolphthalein end point (when the pink color reappeared). Blank titration was also performed with unmodified MFC, and the data was used as a reference. The acetyl content was calculated with the following equation[17]:

$$\text{Acetyl content}(\%) = [(D - C)N_a + (A - B)N_b] \times (4.035) \quad (1)$$

where A is the volume of NaOH added to the sample (mL), B is the volume of NaOH added to the

blank (mL), C is the volume of HCl added to the sample (mL), D is the volume of HCl added to the blank (mL), W is the weight of the sample (g), and N_a and N_b are the normality of the HCl and NaOH solutions, respectively. The average number of acetyl groups per anhydro-D-glucose unit of cellulose (DS) could be calculated from the following equation[24]:

$$\mathrm{DS} = [3.86 \times \mathrm{Acetyl\,content}(\%)]/[102.4 - \mathrm{Acetyl\,content}(\%)] \quad (2)$$

Fourier transform infrared (FTIR) spectroscopy

FTIR spectra of dried samples of acetylated and nonacetylated cellulose were collected with a FTS 600 spectrometer (Bio-Rad Laboratories, Inc., Hercules, CA) equipped with a laser operating at 632.8 nm. The spectra were recorded between 400 and 4000 cm^{-1}. The results were normalized to a height of the band at 1111 cm^{-1} derived from the asymmetric vibrations of C—O and C—C bonds in cellulose (ring breathing).[25–27] The baseline correction was done by the subtraction of a minimum intensity from the spectrum.

Preparation of the composites

PLA was dissolved in chloroform at room temperature under constant agitation for 7 h. The solution had a concentration of 2 wt %. It was mixed with an acetylated MFC suspension in chloroform (1 wt %) to achieve composites with 2, 5, 10, 15, and 20% weight fractions of dry cellulose. The mixture was homogenized for around 2 min and degassed before it was cast onto a glass plate treated with a commercial polymer-based release agent (Chemlease 75, Chem-Trend L. P., Howell, MI). The cast film was kept overnight in a well-ventilated environment at room temperature to allow evaporation of the chloroform. Preparation of the composite films was finalized by placement of the films in an oven at 60°C for 30 min. The films were then removed from the glass plate and conditioned at 50% relative humidity and 23°C. Unreinforced PLA films were prepared in the same way.

Raman imaging

A piece of a stress-free composite film with 2 and 20 wt % loading of MFC was embedded in epoxy resin and left to cure for 24 h at room temperature; this was followed by postcuring for 12 h at 60°C. The epoxy block was microtomed to prepare a smooth surface for Raman imaging. A Nikon 20× objective lens (Tokyo, Japan) was used for imaging. The spatial resolution was 1 μm, and a laser, polarized horizontally and with a wavelength of 532.24 nm (Nd : YAG), was employed. The alpha 300R Confocal Raman microscope (Witec GmbH, Ulm, Germany) was equipped with an Electron Multiplying Charge Coupled Device (EMCCD) camera behind a 600 lines/mm grating. A rectangular area of the surface of the composite film with dimensions of 150 × 10 μm^2 was scanned. An integration time of 0.7 s was used for each spectrum. The Raman images were constructed with characteristic Raman band heights of cellulose (1095 cm^{-1}) and PLA (1130 cm^{-1}). Further details regarding the Raman imaging technique used in this study can be found in a publication by Hänninen et al.[28]

Mechanical testing

Specimens for tensile testing were prepared in accordance with ISO 527 : 1996. Specimen type 1BA was chosen because the size of composites was limited. The specimens were punched out of the films with a custom-made cutting die. There were at least seven specimens in each group. The average film thickness was 70 μm. Specimens were conditioned in accordance with EN ISO 291:2008 at 23 ±1°C and 50 ± 2% relative humidity before the testing. Testing was conducted on an MTS 400/M (Eden Prairie, MN, USA) testing machine situated in the same controlled environment. The testing speed was 5 mm/min and a load cell of 50 N was used. The strain was calculated from the displacement of the crossheads. Analysis of variance was performed to compare means at a significance level of 0.05.

Scanning electron microscopy (SEM)

Fractured tensile specimens were gold sputtered in a BAL-TEC SCD 050 sputter coater (Capovani Brothers, Inc., Scotia, NY) at 40 mA current for 15 s. Then, the cross sections were imaged with a Zeiss supra 40 scanning electron microscope (Carl Zeiss AG, Germany) equipped with a Schottky electron gun (Carl Zeiss AG) and an in-lens secondary electrons detector.

RESULTS AND DISCUSSION

MFC morphology, acetyl content, and FTIR spectroscopy results

The MFC suspension in water consisted of the mixture of fibrils, which varied in length and width (Fig. 2).

The diameters varied between about 10–20 nm and had lengths from 200 nm up to 2–3 μm; this gave rise to aspect ratios ranging from about 20 to about 150. The height profile provided similar data about the fibril width to the widths measured directly from the AFM image. Unlike the MFC used

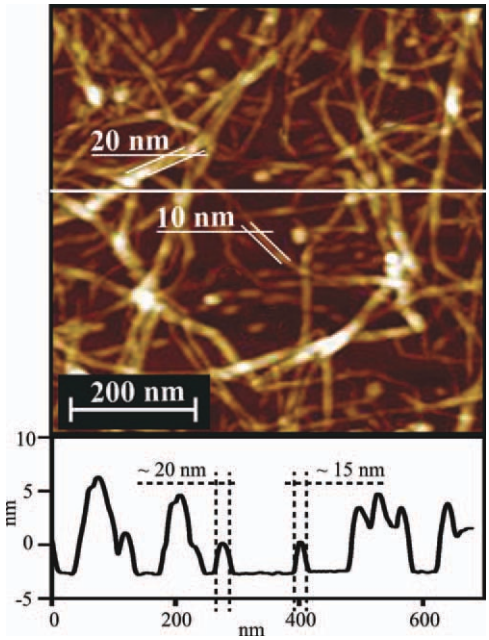

Figure 2 AFM topography image of the spin-coated supernatant of MFC. The height profile of the marked area (white line) is at the bottom of the image. [Color figure can be viewed in the online issue, which is available at wileyonlinelibrary.com.]

for the AFM imaging, the MFC used for composites preparation was not centrifuged and was made up of a mixture of both microfibrils and nanofibrils.

The acetyl contents determined by saponification were 5.9% after 15 min of reaction time and 10.3% after 30 min of reaction time. When eq. (2) was applied, this translated to DS values of 0.24 and 0.43, respectively. The FTIR spectra obtained from the nonacetylated and acetylated MFC samples are presented in Figure 3.

The intensity at approximately 1740 cm^{-1} corresponded to carbonyl (C=O) stretching vibrations.[26,29] The appearance of this band indicated the

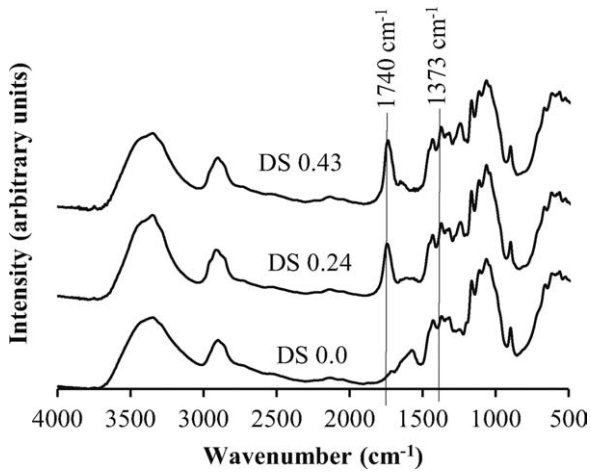

Figure 3 FTIR spectra of the nonacetylated and acetylated MFC with respect to the DS.

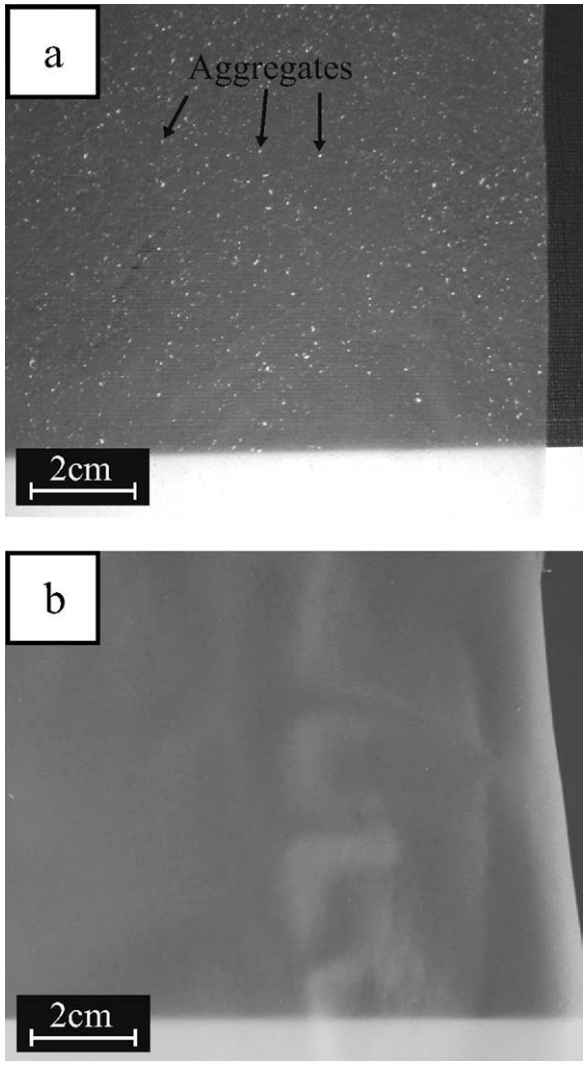

Figure 4 Photographs of the PLA/MFC composites with 20 wt % MFC loading: DS = (a) 0.24 and (b) 0.43.

presence of acetyl groups resulting from the acetylation of accessible primary hydroxyl groups. In addition, the intensity of the band at 1373 cm^{-1}, corresponding to methyl C—H symmetric bending,[26,30] agreed with the increase in DS. However, the technique was not quantitative because of the presence of hemicelluloses (MFC was prepared from birch pulp). The FTIR data aligned with the results obtained by saponification, strongly supporting the contention that the MFC was modified.

Composite morphology and Raman imaging

The dispersion of reinforcing agent was evaluated visually and with a Raman mapping technique. Figure 4 shows the macromorphology of the composite films.

The dispersion of MFC in the PLA matrix was strongly affected by the DS. Cellulose aggregates, visible as white dots, are marked with arrows in

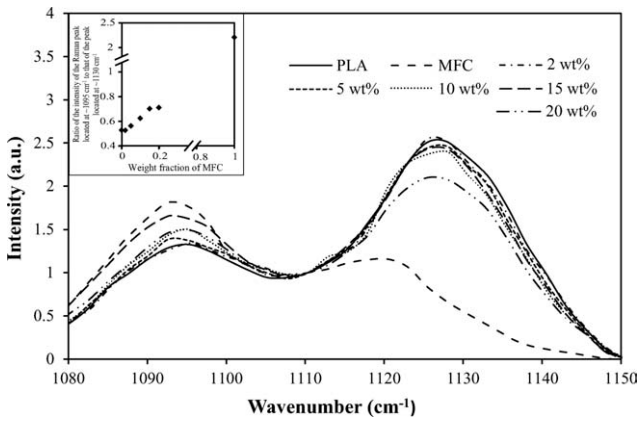

Figure 5 Typical Raman spectra of the pure MFC film, pure PLA film, and composites with 2, 5, 10, 15, and 20 wt % acetylated (DS = 0.43) MFC. The inset shows the ratio of the intensity of the Raman peak located at about 1095 cm^{-1} to that of the peak located at about 1130 cm^{-1} as a function of the weight fraction of acetylated (DS = 0.43) MFC.

Figure 4(a). The preparation of the composites by solvent casting from a nonpolar matrix and polar reinforcement such as cellulose is virtually impossible because polar entities attract each other and form aggregates.[11,31] The acetylation of cellulose hydroxyl groups proved to be an effective way of decreasing polarity and, in turn, improving compatibility with the nonpolar PLA. However, a DS of 0.24 was insufficient to prevent severe aggregation [Fig. 4(a)], most probably because of intermolecular hydrogen bond formation. A far more effective dispersion was achieved at a DS of 0.43 because no visible aggregates could be detected [Fig. 4(b)].

Raman imaging provided some insight into the microscale dispersion of MFC within the PLA matrix. The Raman band located at about 1130 cm^{-1} was characteristic of PLA, and the band located at about 1095 cm^{-1} was characteristic of cellulose,

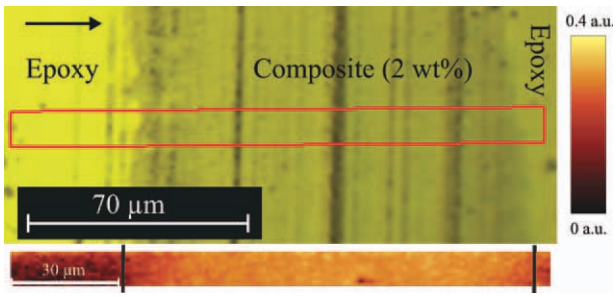

Figure 6 Microscope image of a 2 wt % MFC (DS = 0.43) composite film embedded in the epoxy matrix and a Raman image (bottom) representing the area within the rectangle. The scale bar is on the right-hand side. The vertical black lines denote the boundaries of the composite film. The arrow indicates the polarization direction of the laser. [Color figure can be viewed in the online issue, which is available at wileyonlinelibrary.com.]

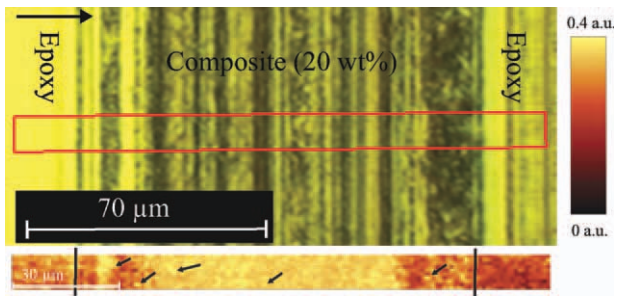

Figure 7 Microscope image of a 20 wt % MFC (DS 0.43) composite film embedded in the epoxy matrix and a Raman image (below) representing the area within the rectangle. The scale bar is on the right-hand side. The vertical black lines denote the boundaries of the composite film. The arrow indicates the polarization direction of the laser. [Color figure can be viewed in the online issue, which is available at wileyonlinelibrary.com.]

although there was a small peak located at about 1095 cm^{-1} due to PLA, this was not thought to affect the positioning of the cellulose band as its intensity significantly increased with the addition of cellulose[32] (Fig. 5).

The relative band intensities corresponding to MFC and PLA changed with respect to the weight fraction of cellulose. The ratio of the intensity of the Raman band located at about 1095 cm^{-1} to the intensity of the band located at about 1130 cm^{-1} plotted against the weight fractions of MFC is shown in the inset in Figure 5. The difference in the intensity ratio increased as the weight fraction of MFC grew. Thus, it provided a potential method for determining the variability within the sample to a spatial resolution of 1–2 µm (the approximate size of the laser spot). The spectra could be collected together and used to construct a chemical map. Each pixel in the Raman image represented the intensity ratio of the characteristic bands. The Raman images (Figs. 6 and 7) show the intensity ratio of the 1095- and 1130-cm^{-1} bands, corresponding to the cellulose/PLA ratio. The lighter color indicates a larger amount of cellulose with respect to PLA.

The low variation in color in the Raman image (Fig. 6) indicates a relatively constant MFC/PLA ratio and implies a good dispersion of MFC within the PLA matrix (the darker region accounting for around 30 µm on the left-hand side of Fig. 7 is the epoxy in which the film was embedded).

As with the Raman image shown in Figure 6, the scanned area in Figure 7 extends on either side, beyond the boundaries of the composite film, by around 15 µm and were, thus, excluded from the analysis. As the scale bar denotes, the lighter color corresponds to a higher amount of cellulose. As expected, because of the higher amount of cellulose in the 20 wt % composite, the Raman image shown in Figure 7 appears lighter in comparison to the

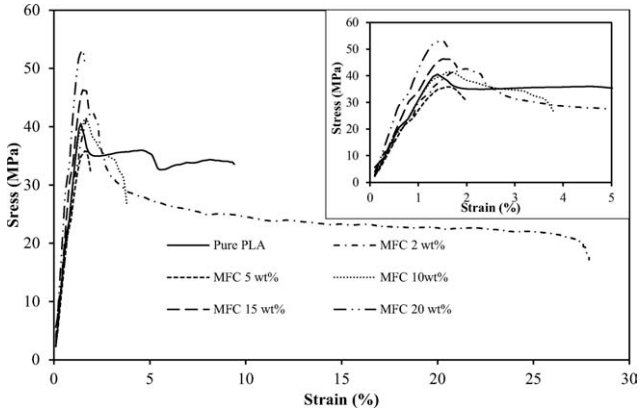

Figure 8 Representative stress–strain curves of the pure PLA and PLA/MFC composites (DS = 0.24). The stress–strain curves in a region below 5% of strain are depicted in the inset.

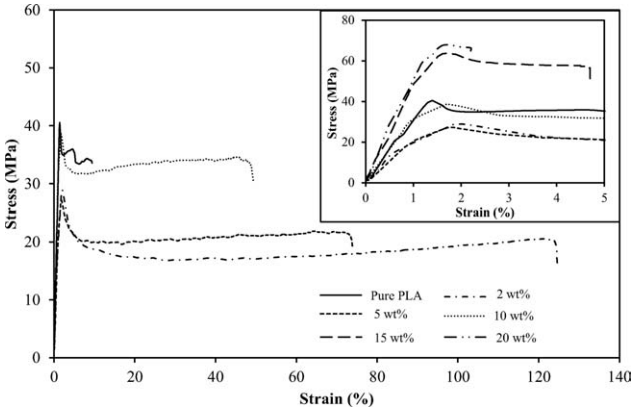

Figure 9 Representative stress–strain curves of the pure PLA and PLA/MFC composites (DS = 0.43). The stress–strain curves in a region below 5% of strain are depicted in the inset.

image shown in Figure 6 (2 wt % composite). The dispersion of cellulose was relatively even in both cases. However, some clustered areas (which are denoted by arrows in Fig. 7) were observed in the 20 wt % loading composite. This may have been due to phase separation because, at the moment of casting, the solution concentration was 2 wt %. Although it seemed that the cellulose concentration in the center of the film was slightly higher, it remained relatively well dispersed because no large distinct aggregates were seen.

Fracture mechanisms and mechanical properties

The stress–strain curves in Figures 8 and 9 show the different mechanical behaviors of the MFC-reinforced composites with respect to the pure PLA film.

A slight inflection in the stress–strain curve of PLA at approximately 5% strain is shown in Figure 8. This may have been the result of slight variations in the sample thickness, with yielding starting earlier in the thinner areas. Cold drawing started simultaneously below 2% strain at several points (Fig. 8), whereas the inflection corresponded to a point where pronounced necking began; this was followed by further cold drawing until fracture. The addition of acetylated cellulose effectively altered the mechanical behavior of the films. No inflection was observed in the stress–strain curves of the composites (Fig. 9), and necking was not pronounced (Fig. 10).

The strain at break and the work of fracture (Table I), expressed as the tensile energy absorbed (TEA), of the composites reinforced with MFC having a DS of 0.43 increased significantly at weight fractions of 10% and below; the strain at break was around 1000% greater (Fig. 9), and the work of fracture was about 600% larger at 2 wt % MFC.

This significant modification to the properties PLA has, to the best of our knowledge, not hitherto been reported. In the composite reinforced with MFC acetylated to a DS of 0.43, the TEA values were greater compared to that of the pure PLA film at reinforcement levels of 5 and 10 wt %. The latter also exhibited a 15% improvement in Young's modulus (Fig. 11);

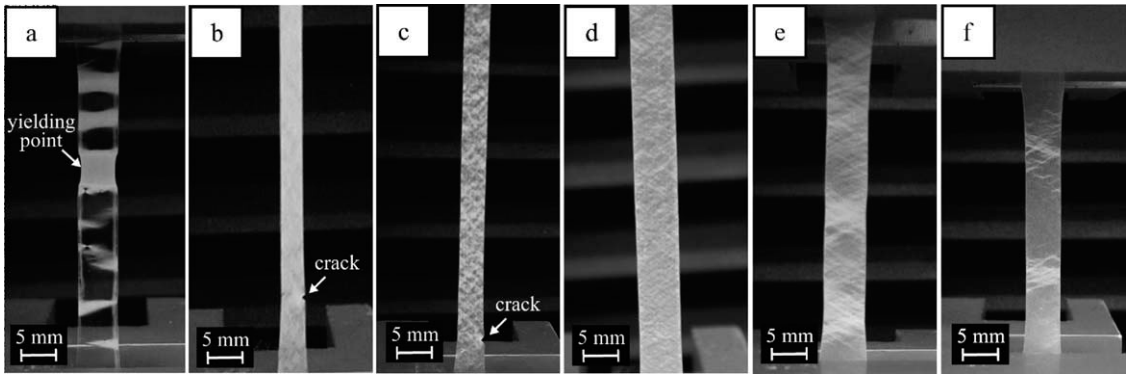

Figure 10 Crazing in the (a) pure PLA film and in acetylated cellulose (DS = 0.43) reinforced composites with different weight fractions: (a) 0, (b) 2, (c) 5, (d) 10, (e) 15, and (f) 20%. The images were taken right before fracture; therefore, the strains were close to the ultimate strain at break, approximately (a) 9.5, (b) 120, (c) 70, (d) 45, (e) 4, and (f) 2%.

TABLE I
TEA and Strain at Break Values of the Composite Films with Respect to the MFC Loading and DS

		MFC wt % (DS)										
		0	2 (0.24)	2 (0.43)	5 (0.24)	5 (0.43)	10 (0.24)	10 (0.43)	15 (0.24)	15 (0.43)	20 (0.24)	20 (0.43)
N^a		15	9	7	7	7	8	6	8	7	8	8
TEA (kJ/m^2)	Average	151	379	1162	76.1	915	59.7	898	37.3	123	37.7	56.1
	SD	113	173	612	72.4	70.2	25.4	95	18.3	59.7	13.0	34.3
Strain at break (%)	Average	8.4	28.5	107	5.2	76.1	3.7	49.4	1.9	4.3	1.9	2.2
	SD	6.0	13.3	49	4.8	5.0	1.4	4.2	0.6	1.7	0.4	0.9

SD, standard deviation.
[a] *N*, number of samples.

thus, the composite was both a tough and a stiff material. There was no significant change in either TEA or in the strain at break for composites reinforced with MFC with a 0.24 DS.

It is known that better dispersion of the reinforcing agent and improved fiber–matrix interaction lead to an enhancement in the mechanical properties of composites. As the mechanical property results suggest, this could be achieved through tailoring of the surface through chemical modification because the properties appear to be extremely sensitive to DS level. However, at higher MFC loadings, the behavior of the composites was similar, regardless of the DS level; this indicated the formation of a rigid structure due to percolation. The results reported herein vary compared to other literature reports. For instance, PLA reinforced with cellulose nanofibers prepared from kenaf pulp showed slight improvements in the Young's modulus and tensile strength at 1, 3, and 5 wt % loadings followed by a decrease in the strain at break.[33] However, the films were prepared by an extrusion method, and no chemical modification was used; some aggregates were, therefore, visible, even at a 1 wt % loading of cellulose. In another study,[21] the addition of acetylated bacterial cellulose (BC) to PLA also led to slightly increased mechanical properties and decreased strains at break at 1, 4, and 6 wt % loadings of acetylated BC. These composites were prepared by injection molding, and the DS of acetylated BC was 0.02; this would have

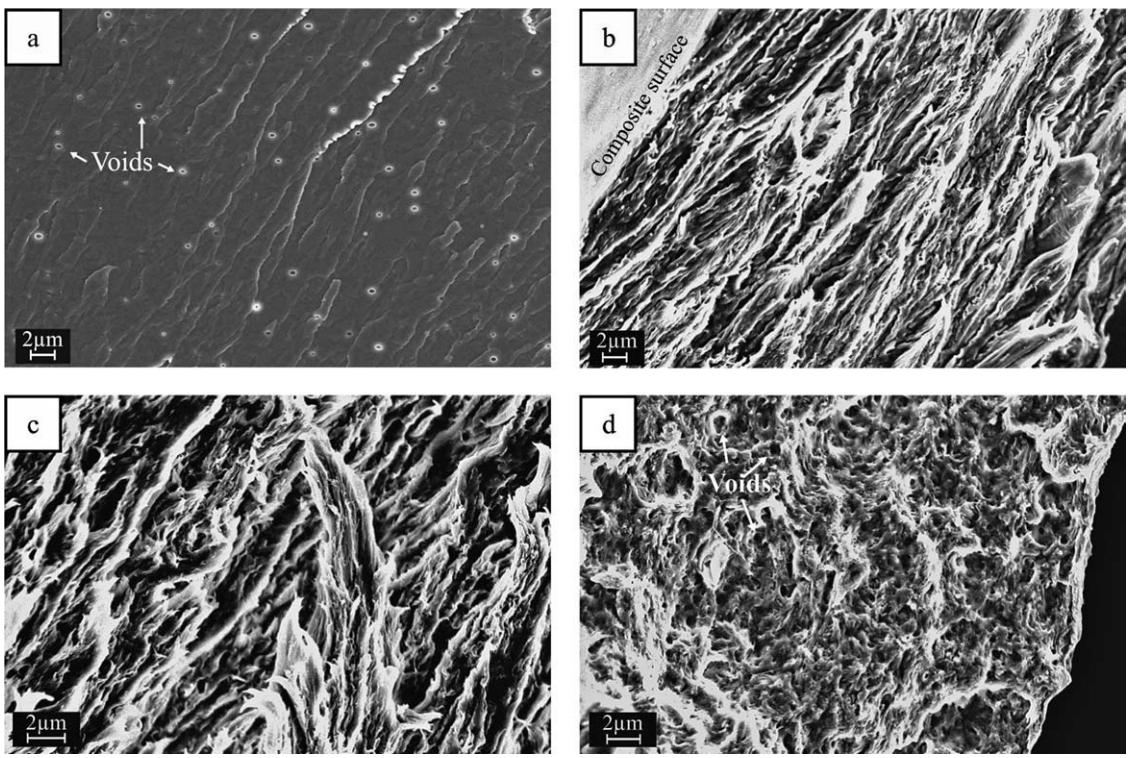

Figure 11 SEM micrographs of the composites fracture surfaces of the (a) pure PLA, (b) 2 wt % MFC, (c) 5 wt % MFC, and (d) 20 wt % MFC (DS of MFC = 0.43).

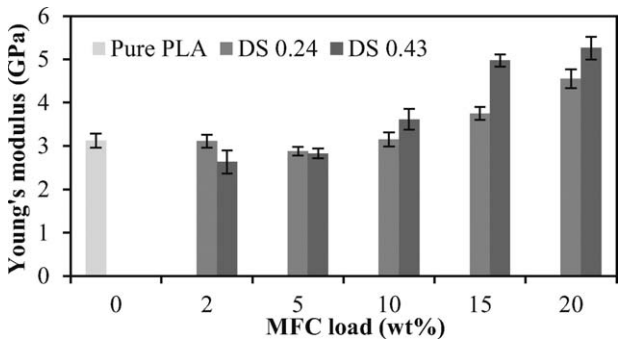

Figure 12 Young's modulus values of the composite films with respect to the MFC loading and DS. The error bars denote the standard deviations. (The values and standard deviations are presented in the Appendix).

led to composite microstructures dissimilar to the ones described herein. Silylated cellulose nanocrystals have been reported to moderately strengthen poly(L-lactide) matrices at loadings of 1 and 2 wt %.[34] However, the cotton nanocrystals used in the study were essentially different from the MFC used herein in terms of morphology.

The addition of cellulose contributed to the distribution of stress throughout the specimen as the stress whitening, the formation of crazes, and voids indicated (Fig. 10). Shear yielding, resulting from a difference in the Young's modulus values of the cellulose and PLA, could have contributed to the transfer of stress and energy dissipation, as shear yielding theory suggests.[35] The reinforcement agent acted as a stress concentrator and caused a stress field. If the stress fields from neighboring inclusions overlapped, shear yielding would have expanded further.

The development of crazes into cracks can be effectively controlled by cellulose fibrils, provided that the interfacial adhesion is good. Thus, crazing and shear yielding were likely contributors to the high values of strain at break reported here. The strain at break values of the composites with below 15 wt % loading of MFC with a DS 0.43 were significantly higher compared to that of pure PLA film. As the MFC weight fraction increased, percolation took place; this resulted in a rigid structure and, finally, yielded brittle composites [Fig. 11(f)].

The brittle nature of PLA fracture has been widely reported.[2,36–38] This can be seen in the SEM micrograph of pure PLA [Fig. 11(a)], which shows little evidence of plastic deformation. The circular features several hundred nanometers in diameter seen in Figure 11(a) could have been the result of either contaminants, such as dust particles, or it could have been voids, resulting from the solvent casting preparation method. Nevertheless, they did not appear to affect the final mechanical properties of the PLA because these were close to the mechanical properties reported by the manufacturer.

The number of small voids present on the fracture surface of the 20 wt % composite [Fig. 11(d)] suggested that crack propagation within the material was due to the extensive formation of voids. In contrast, the fracture surface of the composites with lower loadings of MFC [Fig. 11(b,c)] exhibited a more fibrillar fracture; this indicated pronounced crazing.[39] Interfibril debonding and nanofibril slippage have been reported[40] to be facilitated by voids in pure cellulose structures. The toughness of these films depended on the porosity and the degree of polymerization.[40] This suggested that similar effects could be observed in the MFC/PLA composites where interfibrilar debonding and slippage were additionally facilitated by the lower number of hydrogen bonds because of esterification.

Figure 12 shows the Young's modulus as a function of MFC loading and DS. As shown, both the MFC loading and DS significantly altered the mechanical properties of the composites (see the Appendix).

The Young's modulus of the composites reinforced with MFC having a DS of 0.24 did not show any significant change in stiffness up to 15 wt % loading, whereas the composites reinforced with MFC with a DS of 0.43 exhibited slight reductions in stiffness at 2 and 5 wt % loading of MFC. Interestingly, an analogous trend was reported when a polar matrix (PVA) was reinforced with MFC.[41] A similar decrease was also reported at 1, 2, 3, and 5 wt % loadings of freeze-dried cellulose nanowhiskers in PLA.[2] However, Lin et al.[16] observed an increase in the Young's modulus and tensile strength at a 1 wt % loading of freeze-dried acetylated nanocrystals. The aspect ratios were about 2–15 and about 20–30, respectively; this implied that the morphology of the reinforcing agent played a key role and affected the percolation threshold. In composites reinforced with a 10 wt % loading of MFC having a DS of 0.43, the Young's modulus was improved by 15%. The greatest stiffness enhancement was achieved at a 20 wt %

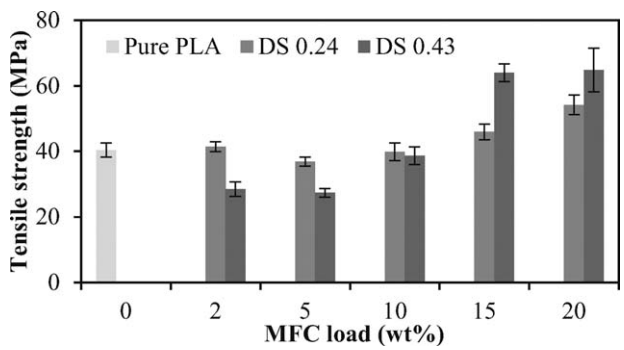

Figure 13 Tensile strength values of the composite films with respect to the MFC loading and DS. The error bars denote the standard deviations. (The values and standard deviations are presented in the Appendix).

loading with increases in the Young's modulus of approximately 50 and 70% for 0.24 and 0.43 DSs, respectively.

Similarly, the tensile strength was affected by the weight fraction of MFC and the DS (Fig. 13).

As shown, the tensile strength of the composite films reinforced with MFC acetylated to a DS of 0.43 exhibited slight decreases at 2 and 5 wt % loadings compared to that of the pure PLA film. In the case of MFC having a DS of 0.24, no difference in the tensile strength was observed at a 2 wt % loading, and only a slight decrease was detected at 5 wt %. The tensile strength of the composites was equal to that of the pure PLA film at 10 wt % loading of acetylated MFC at both levels of DS. This was followed by increases with the 15 and 20 wt % MFC loadings, with a peak at 20 wt %, which resulted in an increase of 60% in tensile strength at a DS of 0.43 and a 35% increase at a DS of 0.24. Discrepancies in the mechanical properties of the composites with respect to DS were most likely due to the tendency of MFC with the lower DS to aggregate. Moreover, the dispersion of MFC with a DS of 0.43 was better at higher MFC loadings (Fig. 4); this led to significantly improved mechanical properties (Figs. 12 and 13).

CONCLUSIONS

The morphology of MFC was studied with AFM, and acetylation was evaluated with the Eberstadt method and FTIR spectroscopy. Raman spectroscopy was employed as a tool to study the distribution of the phases within the composites at a microscale. Thus, it was possible to assess the dispersion of MFC within the PLA matrix. The addition of acetylated MFC significantly altered the fracture mode of the composites films. The DS of MFC played an important role in altering of the mechanical properties, mainly because of better dispersion and because the aggregation of MFC was impeded with a higher DS. There was no change in the Young's modulus up to 10 wt % loading of MFC having a DS of 0.24, whereas the composites reinforced with MFC having a DS of 0.43 exhibited decreases in the Young's modulus at 2 and 5 wt % loadings. Nevertheless, the strain at break and work of fracture increased by approximately 1000 and 650%, respectively, at a 2 wt % loading. This was considered to be mainly due to nucleated crazing upon the addition of MFC. High toughness, expressed as TEA, and stiffness (Young's modulus) were recorded for composites that had a cellulose content of 10 wt %,; these provided both a tough and a strong composite material. Dramatic increases in the strain at break and work of fracture opened up the possibility of new application fields for the PLA composites. This work has shown that it is possible to impart new properties to PLA with the addition of MFC.

The authors thank Rita Hatakka for recording the FTIR spectra, Anna Olszewska for help with the AFM images, and Alexander Perros for help with the SEM imaging. Many thanks are also due to the research group of Jouni Paltakari for providing MFC. The authors acknowledge Tuomas Hänninen for valuable discussions regarding cellulose chemistry and spectroscopy.

APPENDIX

TABLE A.I.
Statistical Significance of the Mean Differences

	MFC wt % (DS)										
	0	2 (0.24)	2 (0.43)	5 (0.24)	5 (0.43)	10 (0.24)	10 (0.43)	15 (0.24)	15 (0.43)	20 (0.24)	20 (0.43)
0		–[c] –[d]	+ +	– –	+ +	– –	+ +	– –	– –	– –	– –
2 (0.24)	–[a] –[b]		+ +	– –	+ +	+ +	+ –	+ +	– –	+ +	– –
2 (0.43)	+ +	+ +		+ +	– +	+ +	– +	+ +	+ +	+ +	+ +
5 (0.24)	– +	– +	– +		+ +	– –	+ +	– –	– –	– –	– –
5 (0.43)	+ +	+ +	– –	– +		+ +	– –	+ +	+ +	+ +	+ +
10 (0.24)	– –	– –	+ +	– –	+ +		+ +	– –	– –	– –	– –
10 (0.43)	+ –	+ –	+ +	+ –	+ +	+ –		+ +	+ +	+ +	+ +
15 (0.24)	+ +	+ +	+ +	+ +	+ +	+ +	– +		– –	– –	– –
15 (0.43)	+ +	+ +	+ +	+ +	+ +	+ +	+ +	+ +		– –	– –
20 (0.24)	+ +	+ +	+ +	+ +	+ +	+ +	+ +	+ +	+ +		– –
20 (0.43)	+ +	+ +	+ +	+ +	+ +	+ +	+ +	+ +	– –	+ +	

+, the mean difference was significant at the 0.05 level; –, the mean difference was not significant at the 0.05 level.
[a] Young's modulus.
[b] Tensile strength.
[c] TEA.
[d] Strain at break.

TABLE A.II.
Tensile Strength and Young's Modulus Values of the MFC/PLA Composite Films

MFC wt % (DS)		0	2 (0.24)	2 (0.43)	5 (0.24)	5 (0.43)	10 (0.24)	10 (0.43)	15 (0.24)	15 (0.43)	20 (0.24)	20 (0.43)
N^a		15	9	7	7	7	8	6	8	7	8	8
Tensile strength (MPa)	Average	40.4	41.4	28.5	36.9	27.4	39.9	38.7	45.9	64.0	54.2	64.8
	SD	2.2	1.5	2.2	1.3	1.3	2.7	2.7	2.5	2.7	3.0	6.7
Young's modulus (GPa)	Average	3.1	1.1	2.6	2.9	2.8	3.1	3.6	3.7	5.0	4.6	5.3
	SD	0.2	0.03	0.27	0.1	0.1	0.2	0.2	0.2	0.1	0.2	0.3

SD, standard deviation.
[a] Number of samples.

References

1. Garlotta, D. J Polym Environ 2001, 9, 63.
2. Sanchez-Garcia, M.; Lagaron, J. Cellulose 2010, 17, 987.
3. Okubo, K.; Fujii, T.; Thostenson, E. T. Compos A 2009, 40, 469.
4. Gabr, M. H.; Elrahman, M. A.; Okubo, K.; Fujii, T. Compos Struct 2010, 92, 1999.
5. Gabr, M.; Elrahman, M.; Okubo, K.; Fujii, T. J Mater Sci 2010, 45, 3841.
6. Gabr, M. H.; Elrahman, M. A.; Okubo, K.; Fujii, T. Compos A 2010, 41, 1263.
7. Faber, K. T.; Evans, A. G. Acta Metall 1983, 31, 565.
8. Sakurada, I.; Nukushina, Y.; Ito, T. J Polym Sci 1962, 57, 651.
9. Sturcova, A. Biomacromolecules 2005, 6, 1055.
10. Iwamoto, S.; Kai, W.; Isogai, A.; Iwata, T. Biomacromolecules 2009, 10, 2571.
11. Heux, L.; Chauve, G.; Bonini, C. Langmuir 2000, 16, 8210.
12. Siqueira, G.; Bras, J.; Dufresne, A. Biomacromolecules 2009, 10, 425.
13. Kim, D.; Nishiyama, Y.; Kuga, S. Cellulose 2002, 9, 361.
14. Ifuku, S.; Nogi, M.; Abe, K.; Handa, K.; Nakatsubo, F.; Yano, H. Biomacromolecules 2007, 8, 1973.
15. Çetin, N. S.; Tingaut, P.; Özmen, N.; Henry, N.; Harper, D.; Dadmun, M.; Sèbe, G. Macromol Biosci 2009, 9, 997.
16. Lin, N.; Huang, J.; Chang, P. R.; Feng, J.; Yu, J. Carbohydr Polym 2011, 83, 1834.
17. Tingaut, P.; Zimmermann, T.; Lopez-Suevos, F. Biomacromolecules 2010, 11, 454.
18. Liu, D. Y. Express Polym Lett 2010, 4, 26.
19. Iwatake, A.; Nogi, M.; Yano, H. Compos Sci Technol 2008, 68, 2103.
20. Takatani, M.; Ikeda, K.; Sakamoto, K.; Okamoto, T. J Wood Sci 2008, 54, 54.
21. Tome, L. C.; Pinto, R. J. B.; Trovatti, E.; Freire, C. S. R.; Silvestre, A. J. D.; Neto, C. P.; Gandini, A. Green Chem 2011, 13, 419.
22. Nogi, M.; Abe, K.; Handa, K.; Nakatsubo, F.; Ifuku, S.; Yano, H. Appl Phys Lett 2006, 89, 233123.
23. Okahisa, Y.; Yoshida, A.; Miyaguchi, S.; Yano, H. Compos Sci Technol 2009, 69, 1958.
24. Tanghe, L. J.; Genung, L. B.; Mench, W. J. In Methods in Carbohydrate Chemistry; Whistler, R. L., Green, J. W., BeMiller, J. N., Wolfrom, M. L., Eds.; Academic: London, 1963; p 201.
25. Nelson, M. L.; O'Connor, R. T. J Appl Polym Sci 1964, 8, 1311.
26. Kondo, T.; Sawatari, C. Polymer 1996, 37, 393.
27. Schenzel, K.; Fischer, S. Cellulose 2001, 8, 49.
28. Hänninen, T.; Kontturi, E.; Vuorinen, T. Phytochemistry 2011, 72, 1889.
29. Guo, Y.; Wu, P. Carbohydr Polym 2008, 74, 509.
30. Colom, X.; Carrillo, F. Eur Polym J 2002, 38, 2225.
31. Ljungberg, N.; Bonini, C.; Bortolussi, F.; Boisson, C.; Heux, L.; Cavaillé, J. Y. Biomacromolecules 2005, 6, 2732.
32. Quero, F.; Nogi, M.; Yano, H.; Abdulsalami, K.; Holmes, S. M.; Sakakini, B. H.; Eichhorn, S. J. Am Chem Soc Appl Mater Interfaces 2010, 2, 321.
33. Jonoobi, M.; Harun, J.; Mathew, A.; Hussein, M.; Oksman, K. Cellulose 2010, 17, 299.
34. Pei, A.; Zhou, Q.; Berglund, L. A. Compos Sci Technol 2010, 70, 815.
35. Liang, J. Z.; Li, R. K. Y. J Appl Polym Sci 2000, 77, 409.
36. Mathew, A. P.; Oksman, K.; Sain, M. J Appl Polym Sci 2005, 97, 2014.
37. Oksman, K.; Mathew, A. P.; Bondeson, D.; Kvien, I. Compos Sci Technol 2006, 66, 2776.
38. Suryanegara, L.; Nakagaito, A. N.; Yano, H. Compos Sci Technol 2009, 69, 1187.
39. Hull, D. Fractography: Observing, Measuring and Interpreting Fracture Surface Topography; Cambridge University Press: Cambridge, United Kingdom, 1999; p 366.
40. Henriksson, M.; Berglund, L. A.; Isaksson, P.; Lindström, T.; Nishino, T. Biomacromolecules 2008, 9, 1579.
41. Bulota, M.; Jäskeläinen, A.; Paltakari, J.; Hughes, M. J Mater Sci 2011, 46, 3387.